

Automated Plant Disease Recognition using Tasmanian Devil Optimization with Deep Learning Model

^{1,*}N. Venkatakrisnan, ²M. Natarajan

¹Research Scholar, Department of Computer and Information Science,
Annamalai University, Annamalai Nagar - 608 002.
narayananv175@gmail.com

²Assistant Professor/Programmer, Department of Computer and Information Science,
Annamalai University, Annamalai Nagar - 608 002.
mind.2004@gmail.com

Abstract—Plant diseases have devastating effects on crop production, contributing to major economic loss and food scarcity. Timely and accurate recognition of plant ailments is vital to effectual disease management and keeping further spread. Plant disease classification utilizing Deep Learning (DL) has gained important attention recently because of its potential to correct and affect the detection of plant diseases. DL approaches, particularly Convolutional Neural Networks (CNNs) demonstrate that extremely effective in capturing intricate patterns and features in plant leaf images, allowing correct disease classification. In this article, a Tasmanian Devil Optimization with Deep Learning Enabled Plant Disease Recognition (TDODL-PDR) technique is proposed for effective crop management. The TDODL-PDR technique derives feature vectors utilizing the Multi-Direction and Location Distribution of Pixels in Trend Structure (MDLDPTS) descriptor. Besides, the deep Bidirectional Long Short-Term Memory (BiLSTM) approach gets exploited for the plant disease recognition. Finally, the TDO method can be executed to optimize the hyperparameters of the BiLSTM approach. The TDO method inspired by the foraging behaviour of Tasmanian Devils (TDs) effectively explores the parameter space and improves the model's performance. The experimental values stated that the TDODL-PDR model successfully distinguishes healthy plants from diseased ones and accurately classifies different disease types. The automated TDODL-PDR model offers a practical and reliable solution for early disease detection in crops, enabling farmers to take prompt actions to mitigate the spread and minimize crop losses.

Keywords- Automated plant disease recognition, Tasmanian devil optimization, deep learning model, hyperparameter optimization, crop management

I. INTRODUCTION

Infections in plants are among the major essential factors affecting crop productivity. It is more liable for a considerable reduction in the crop economic production and being a barrier to these activities in a few conditions [1]. The disease control and management methods should be implemented efficiently to decrease the production losses and make sure agricultural viability, highlighting the significance of continuous crop observation matched with prompts and effectively detecting the diseases [2]. Moreover, as the global population constantly increases, a substantial improvement in the production of foods is mandatory (FAO) [3]. This should be together with the protection of the natural ecosystem through the usage of environment-friendly agriculture techniques [4]. Foods should maintain a higher nutritional value while even being protective globally. This could be achieved by the use of recent scientific technologies for managing the crop and diagnosing plant diseases for monitoring large-scale ecosystems [5].

The concepts of conventional disease management techniques need manual exploration of areas, which leads to delayed crop disease examination [6]. Additionally, conventional techniques are subjective because of visual analysis by professional plant pathologists. To resolve the drawbacks offered by conventional crop disease analysis, rapid and efficient disease recognition methods were proposed with computer vision-based image analysis [7]. Nevertheless, many solutions are dependent on feature engineering to describe the needed features related to every individual disease. Hence, based on DL has been newly raised to design generalized results [8]. DL has acquired popularity within the earlier ten-year period because of technical development in the databases availabilities, Graphical Processing Units (GPUs), and memory capacities. The modern technologies to manage plant disease comprises using Deep Neural Networks (DNNs) to automatically acquire features from image training data that are significant for training disease-recognized patterns [9]. This method supports bypass features engineering and features extraction demands when

growing disease managing systems. For the identification of plant disease, DL techniques commonly depend on higher-level features that can be derived from visual symptoms [10]. Thus, accessing effective imagery databases is crucial.

In this article, a Tasmanian Devil Optimization with Deep Learning Enabled Plant Disease Recognition (TDODL-PDR) technique is proposed for effective crop management. The TDODL-PDR technique derives feature vectors utilizing the Multi-Direction and Location Distribution of Pixels in Trend Structure (MDLDPTS) descriptor. Besides, the deep Bidirectional Long Short-Term Memory (BiLSTM) approach gets exploited for the plant disease recognition. Finally, the TDO method can be executed to optimize the hyperparameters of the BiLSTM approach. The TDO method inspired by the foraging behaviour of Tasmanian Devils (TDs) effectively explores the parameter space and improves the model's performance. The experimental values stated that the TDODL-PDR model successfully distinguishes healthy plants from diseased ones and accurately classifies different disease types.

II. LITERATURE REVIEW

Abd Algani et al. [11] suggested a novel DL technique for the recognition and classification of diseases termed ACO-CNN. The efficiency of plant leaf disease recognition was examined by the ACO. Plant leaf arrangement, Geometries of texture, and colour are deducted from the presented images using CNN classifiers. Pal and Kumar [12] developed an Agriculture Detection (AgriDet) architecture, which integrates the Inception-VGG Network (INC-VGGN) and Kohonen-based DL network for detecting plant ailment and classifying the cruelty level of infected vegetation. Now, the pretrained INC-VGGN architecture is a DCNN for predicting plant disease that was trained previously for the distinct datasets.

Reddy et al. [13] introduced a customized PDICNet architecture for classifying and recognizing the Plant Leaf Disease (PLD). At first, ResNet50 is used for extracting different features in plant leaf imageries with texture and colour aspects. Moreover, the Modified Red Deer Optimizer Algorithm (MRDOA) can be performed as an optimum FS to attain maximized and relevant factors with the decreased MRDOA size. Furthermore, a DL-CNN classifier model is used to accomplish better efficiency of classification. Attallah [14] introduces a workflow for the automated detection of tomato leaf disease using 3 compact CNNs. It exploits TL to recover strong features out of ending FC layers of the CNN for high-level and further condensed representation. Then, it combines features in the 3 CNNs to advantage in all the CNN structures. In [15], the Modified InceptionResNetV2 (MIR-V2) is a CNN procedure architecture that was utilized along with the TL method for recognizing illness in images of tomato leaves.

Pandian et al. [16] devised a DCNN architecture for the detection of image-based PLDs utilizing hyperparameter optimization and data augmentation methods. The random search method was used for optimizing the hyperparameter of the presented architecture. This study portrays the criticality of electing a fitting filter and layer numbers in the development of DCNN. The authors [17] introduced an automated mechanism for detecting and classifying PLD utilizing Optimum Mobile Network-based CNN (OMNCNN). Furthermore, the MobileNet architecture has been used as a feature extraction approach but the hyperparameter was enhanced by using the EPO approach to improve the detection rate of plant diseases. At last, to allocate accurate classes to the plant leaf imageries, ELM-based classifiers are utilized in the research.

III. THE PROPOSED MODEL

In the presented article, concentration is provided on the development of the TDODL-PDR technique for the accurate and automated recognition of PLDs. The TDODL-PDR technique mainly aims to accomplish enhanced crop productivity by reducing crop losses. In addition, the TDODL-PDR technique makes use of the MDLDPTS technique for the feature extraction process, and the BiLSTM model is applied for classification purposes. At last, the TDO approach was utilized for the optimal hyperparameter selection of the BiLSTM model. Fig. 1 displays the overall process of the TDODL-PDR method.

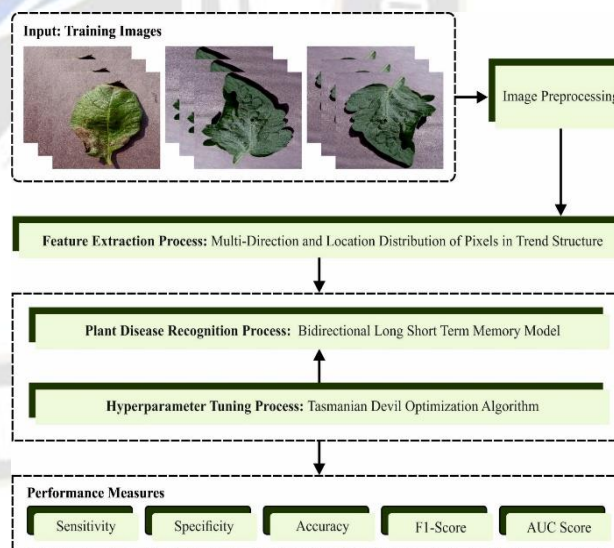


Figure 1. Overall process of TDODL-PDR methodology

A. Modeling of MDLDPTS Description

The study integrated MDLDPTS model that efficiently demonstrates the spatial procedure of local level structure, data pixel alterations, and relationship amongst local level structure in the procedure of small\large\equal trends for shape, texture, and colour signifiers in which small\large\equal trends describe pixel value remain unchanged, small to large and large to small

correspondingly [18]. In addition, MDLDPTS encoded the average location of the pixel distribution value of all the trends in the local level structure.

Transform RGB into the colour space of HSV for exploiting MDLDPTS, then edge quantization on Sobel operator executed V element images, and quantization of texture on V colour on H , S , and V are implemented and the quantization level was set to 9, 108 and 20 for edge, colour and texture data correspondingly. Consequently, a 3×3 non-overlapped window was displaced in left-right orientation from corner position of left-top to right-bottom for all the edge\color\texture quantization data. Local structure for every 3×3 non-overlapping sub-images is evaluated for all the edge\texture\color quantized data in the procedure of trends.

MDLDPTS is a matrix of edge\color\texture quantization value versus orientation of small\large\equal trend structures and edge\color\texture quantized value versus average position for pixel dispersion of small\large\equal trend structures for all the orientations. The calculated edge, colour, and texture features for trend structures and their directions (viz., 0° , 45° , 90° , and 135°) are shown below:

$$F_\theta = \{(\theta_E^{Q_c}, \theta_S^{Q_c}, \theta_L^{Q_c}), (\theta_E^{Q_e}, \theta_S^{Q_e}, \theta_L^{Q_e}), (\theta_E^{Q_t}, \theta_S^{Q_t}, \theta_L^{Q_t})\} \quad (1)$$

In Eq. (1), E , S , and L represent the equivalent, smaller, and larger trends structures, orientation $(\theta) \in \{0^\circ, 45^\circ, 90^\circ, 135^\circ\}$, value of quantized colour $(Q_c) \in \{1, 2, \dots, 108\}$, value of quantization texture $(Q_t) \in \{1, 2, \dots, 20\}$, value of quantization edge $(Q_e) \in \{1, 2, \dots, 9\}$, $\theta_E^{Q_c}$, $\theta_E^{Q_e}$ and $\theta_E^{Q_t}$ correspondingly signifies the orientation of equivalent trends structure for Q_c , Q_e and Q_t . Thus, the dimension of the matrices $\theta_E^{Q_c}$, $\theta_E^{Q_e}$ and $\theta_E^{Q_t}$ are 108×4 , 9×4 and 20×4 . The computed position of pixel distribution for the structure of local level trend is shown below:

$$F_\mu = \{(\mu_{E\theta}^{Q_c}, \mu_{S\theta}^{Q_c}, \mu_{L\theta}^{Q_c}), (\mu_{E\theta}^{Q_e}, \mu_{S\theta}^{Q_e}, \mu_{L\theta}^{Q_e}), (\mu_{E\theta}^{Q_t}, \mu_{S\theta}^{Q_t}, \mu_{L\theta}^{Q_t})\} \quad (2)$$

In Eq. (2), μ refers to the location of distribution for pixel value, $\mu_{E\theta}^{Q_c}$, $\mu_{E\theta}^{Q_e}$ and $\mu_{E\theta}^{Q_t}$ represent the place of dispersion for pixel at θ orientation of equivalent trend structure for Q_c , Q_e and Q_t correspondingly. The computation of μ in every local level structure trend's construction is shown as follows:

$$\mu = \frac{1}{M} \sum_{i=0}^M P_i \quad (3)$$

In Eq. (3), P and M represent the pixels and pixel counts in the trend structure.

$$F = \{F_\theta, F_\mu\} \quad (4)$$

B. Process involved in BiLSTM Model

Once the features are generated, they are fed into the BiLSTM model to classify PLDs. For addressing the vanishing gradients issue in the networks of RNNs, LSTM are presented [19]. It accomplishes this by making a model, which maintains information for a longer time. Memory cells present in the network of LSTM usually comprise self-loops. An input, forget, and output gates can be demonstrated in the imagery as the 3 gates accountable for data flow in the LSTM cell. Reading, writing, and erasing the layers of the memory cell are done using the output, input, and forget gate. A self-loops of the LSTM network permit to save of some sequential data which is encrypted on the layer of the memory cell. Fig. 2 showcases the framework of BiLSTM.

The next formulas define that a single LSTM network cell functions:

$$\left\{ \begin{array}{l} i_g = \sigma(i_{[t]}W_{ix} + o_{[t-1]}W_{im} + b_i) \\ f_g = \sigma(i_{[t]}W_{fx} + o_{[t-1]}W_{fm} + b_f) \\ f_g = \sigma(i_{[t]}W_{ox} + o_{[t-1]}W_{fo} + b_o) \\ u = \tanh(i_{[t]}W_{ux} + o_{[t-1]}W_{um} + b_u) \\ s_{[t]} = (f_g s_{t-1} + i_g \circ u) \\ h_{[t]} = (o_g \circ \tanh(u)) \end{array} \right\} \quad (5)$$

Whereas i_g , 0_g , f_g and exemplify the corresponding inputs of input, output, and forget gates; u denotes the update signal, $s_{[t]}$, and $h_{[t]}$ cell state and output, σ and \tanh define the sigmoid activation and hyperbolic tangent functions, W and b signify the weight and bias matrices of one LSTM cell. Besides, the function of sigmoid activation adapts the value of input as an integer within $[0, 1]$, and also allows complete or null data flow with the gates. The function of hyperbolic tangent activation portrayed as \tanh resolves the vanishing gradient problem, as its subsequent derivative offers an extensive value range before gradually reducing to 0.

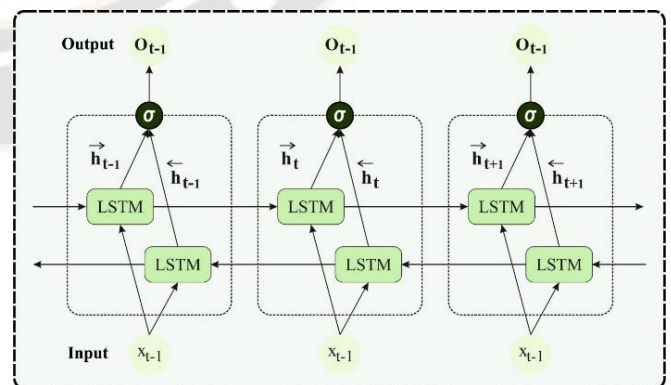


Figure 2. Framework of BiLSTM

LSTM cells are loaded over together to make a multiple or deep layered networking. Thus, every LSTM layer contains many hidden cells. The LSTM layer utilized in this case is bi-

directional because the input series can run both forward and backwards. The count of memory cells is doubled from all the layers of the BiLSTM network. The difference between LSTM and BiLSTM layers is that the second layer remembers and learns data from input in either forward or converse orientations. The forward direction was utilized for remembers previous values of input, but the backward direction will be remembering the values of the future input. At each time step t , either past or future data can be available thanks to the group of 2 Hidden Layers (HLs) storing the data individually (\overleftarrow{h}_t (backward HL) and \overrightarrow{h}_t (forward HL). The last HL h_t is calculated as $h_t = \partial(\overleftarrow{h}_t, \overrightarrow{h}_t)$ that ∂ which could be a process of multiplication, concatenation, average, or summation operation; this integrates the HL series going, forwards \overrightarrow{h}_t and backward \overleftarrow{h}_t . Additionally, the BiLSTM cell results at each phase step t are measured by executing the steady LSTM unit functional formulas as provided in Eq. (5).

C. Design of TDO-based Hyperparameter Optimization

In order optimally choose the hyperparameter of the BiLSTM approach, the TDO technique gets employed. Dehghani et al. [20] presented a bio-motivated method termed TDO that simulators the performance of the TD. TD is a flesh-eating carnivores, a marsupial that belongs to the Dasyuridae family. The feeding process of TDs that is utilized in carnivore eating and live hunting of the prey, is the major motivation for TDO. The TD comprises dissimilar eating methods. The TD exploits the initial approach and feeds it if a carrion is found. The search behaviours of TDs for prey in dissimilar regions disclose the exploration feature in the optimizer technique to select the optimum region of searching spaces. Simultaneously, the TD chases the prey in a constraint area, and this procedure is related to the local searching process that purposes to congregate on the optimum solution by using the issue constraint, a primary search agent populace is produced arbitrarily during the initializing stage. The carrion was chosen, the newest location of the TD in the searching space was defined, and the location of TD was upgraded during the exploration stage. During the exploitation stage, two phases namely attack, prey chasing, and prey selection were modeled [21]. This method was applied to resolve 23 benchmark functions to define the accomplishment quality of the TD optimizer and its performance was compared to dissimilar metaheuristic approaches. The applications, advantages, and disadvantages of GWO, BWO, TDO, and COOT approaches are listed. Pseudocode and Mathematical modelling of TDO is given as follows:

Algorithm 1: Pseudocode of TDO

Read the input variables namely maximal iteration counts and population size.
 Initializing the location of TDs and estimating the main function.
 For $t = 1$ to the Iteration (N),
 For $t = 1$ to the Count of populations.
 If the probability = rand, probability < 0.5.
 Chose the carrion by the i^{th} TD
 $C_i = X_M$
 Where
 $i = 1:N, M \in 1,2,3 \dots N|M \neq i|$
 The strategy of TDs for moving to the newest location is evaluated by:

$$x_{i,j}^{new} = \begin{cases} X_{i,j} + r \cdot (C_{ij} - I \cdot X_{ij}) & , OF_{Ci} < OF_i \\ X_{i,j} + r \cdot (X_{ij} - C_{ij}), & otherwise \end{cases}$$

 Upgrade the location of the i^{th} TD:

$$x_i = \begin{cases} X_i^{new}, OF_i^{new} < OF_i \\ X_i, otherwise \end{cases}$$

 Else.
 The prey is chosen through the TD
 $P_i = X_M$
 Where
 $i = 1:N, M \in 1,2,3 \dots N|M \neq i|$.
 The new location of TDs is evaluated:

$$X_{i,j}^{ne} = \begin{cases} X_{i,j} + r \cdot (P_{ij} - I \cdot X_{ij}) & OF_{Pi} < OF_i \\ X_{i,j} + r \cdot (X_{ij} - P_{ij}) & otherwise \end{cases}$$

 Upgrade the location of the i^{th} TD:

$$X_i = \begin{cases} X_i^{new}, OF_i^{new} < OF_i \\ X_i, otherwise_i \end{cases}$$

 The radius of a neighbourhood where the food hunting happens is evaluated:

$$R = 0.01 \left(1 - \frac{t}{T} \right)$$

 The newest location of TD is dependent upon the chasing procedure and the upgraded location is given as follows.

$$X_{i,j}^{new} = X_{i,j} + (2 * r - 1) \cdot R \cdot X_{i,j}$$

$$X_i = \begin{cases} X_i^{new}, OF_i^{new} < OF_i \\ X_i, otherwise_i \end{cases}$$

 End if.
 Print the better candidate solution. The end for $i = 1$:
 Maximal iteration.
 End.

The TDO system produces a Fitness Function (FF) to accomplish an improved classifier solution. It explains a positive integer to exemplify the best solution for candidate performance. During this case, the lessened error rate of the classifier was supposed that FF, as provided in Eq. (6).

$$fitness(x_i) = ClassifierErrorRate(x_i) = \frac{\text{number of misclassified samples}}{\text{Total number of samples}} * 100 \quad (6)$$

IV. RESULTS AND DISCUSSION

In the current segment, the plant ailment recognition outcome of the TDODL-PDR technique is examined under distinct datasets [22]. Table 1 illustrates the detailed description of various datasets.

A brief set of classification results offered by the TDODL-PDR technique on distinct datasets are portrayed in Table 2. The experimental values pointed out that the TDODL-PDR technique categorized four class labels. On the apple leaves dataset, the TDODL-PDR technique achieves an average $sens_y$ of 99.10%, $spec_y$ of 99.15%, $accu_y$ of 99.11%, F_{score} of 98.86%, and AUC of 99.80%. Simultaneously, on the cherry leaves dataset, the TDODL-PDR method accomplishes an average $sens_y$ of 99.35%, $spec_y$ of 99.29%, $accu_y$ of 99.89%, F_{score} of 98.81%, and AUC of 99.46%. Eventually, on the grape leaves' dataset, the TDODL-PDR method achieves an average $sens_y$ of 96.71%, $spec_y$ of 95.98%, $accu_y$ of 97.93%, F_{score} of 96.03%, and AUC of 96.99%. Meanwhile, on the potato leaves dataset, the TDODL-PDR methodology attains an average $sens_y$ of 96.66%, $spec_y$ of 96.18%, $accu_y$ of 96.11%, F_{score} of 96.08%, and AUC of 96.49%. At last, on the tomato leaves dataset, the TDODL-PDR methodology reaches an average $sens_y$ of 93.95%, $spec_y$ of 94.03%, $accu_y$ of 94.46%, F_{score} of 94.72%, and AUC of 95.95%.

TABLE I. DETAILS OF DATASETS

Classes	No. of Images	Classes	No. of Images
Apple Leaves Dataset		Tomato Leaves	
Healthy	554	Bacterial_Spot	3404
Black Rot	199	Early_Blight	2886
Scab	221	Healthy	516
Cedar Apple Rust	99	Late_Blight	3769
Cherry Leaves Dataset		Leaf_Mold	
Powdery Mildew	409	Septoria_Leaf_Spot	1331
Healthy	334	Spider_Mites	2251
Corn Plant Leaves Dataset		Target_Spot	
Cercosporos-LS	187	Mosaic_Virus	2411
Common Rust	432	Yellow_Leaf_Curl_Virus	2144
Healthy	354	Pepper Leaves Dataset	
Northern Leaf Blight	433	Bacterial Spot	1377

Grape Leaves Dataset		Healthy	1372
Block Rot	407	Potato Leaves Dataset	
Leaf Blight	465	Early Blight	1377
Healthy	146	Late Blight	1372
Esca	379	Healthy	193

TABLE II. CLASSIFICATION OUTCOME OF THE TDODL-PDR APPROACH UNDER VARIOUS DATASETS

Classes	Sensitivity	Specificity	Accuracy	F1-Score	AUC
Apple Leaves Dataset					
Healthy	99.01	99.06	98.23	99.05	99.84
Black Rot	99.01	98.45	99.61	97.69	99.57
Scab	99.08	99.68	99.09	100.72	99.29
Cedar Apple Rust	99.31	99.42	99.50	97.99	100.50
Average	99.10	99.15	99.11	98.86	99.80
Cherry Leaves Dataset					
Powdery Mildew	100.08	100.09	100.63	99.29	99.08
Healthy	98.88	98.62	99.92	98.27	99.51
Average	99.35	99.29	99.89	98.81	99.46
Corn Plant Leaves Dataset					
Cercosporos-LS	97.47	98.27	98.84	96.62	97.93
Common Rust	97.97	97.82	98.15	98.59	97.20
Healthy	98.24	97.98	97.25	96.91	97.75
Northern Leaf Blight	97.25	97.74	98.02	99.39	97.12
Average	97.73	97.95	98.07	97.88	97.50
Grape Leaves Dataset					
Block Rot	98.12	95.92	97.73	96.67	97.85
Leaf Blight	97.41	96.66	96.96	95.97	96.48
Healthy	95.83	95.51	97.23	96.55	95.97
Esca	95.47	95.81	99.80	94.92	97.66
Average	96.71	95.98	97.93	96.03	96.99
Peper Leaves Dataset					
Bacterial Spor	97.02	96.81	99.76	97.13	97.85
Healthy	95.41	96.93	99.66	95.25	97.60
Average	96.22	96.87	99.71	96.19	97.73
Potato Leaves Dataset					
Early Blight	96.02	95.71	95.82	96.35	96.69
Late Blight	97.39	96.91	96.07	95.94	96.84
Healthy	96.58	95.91	96.43	95.94	95.94
Average	96.66	96.18	96.11	96.08	96.49
Tomato Leaves					
Bacterial_Spot	94.40	95.53	93.26	95.27	95.31
Early_Blight	95.78	94.44	92.77	93.75	96.43
Healthy	95.07	95.16	91.94	92.91	95.64

Late_Blight	93.00	93.34	92.51	94.98	94.20
Leaf_Mold	93.86	93.47	95.91	93.06	96.05
Septoria_Leaf_Spot	95.95	93.38	93.32	94.73	95.94
Spider_Mites	95.00	95.08	93.91	93.21	95.76
Target_Spot	93.01	93.60	94.32	95.71	96.40
Mosaic_Virus	94.26	93.58	93.98	95.26	95.04
Yellow_Leaf_Curl_Virus	93.51	93.86	95.63	94.68	96.61
Average	93.95	94.03	94.46	94.72	95.95

In Fig. 3, a ROC curve of the TDODL-PDR approach is exposed on various databases. The outcome defined that the TDODL-PDR approach led to superior ROC values. In addition, it can be obvious that the TDODL-PDR methodology is extend greater ROC values in 11 class labels.

Table 3 and Fig. 4, a widespread relative research of the TDODL-PDR technique with current approaches with regard to distinct metrics. The results inferred that the TDODL-PDR technique obtains improved performance on all datasets. Concurrently, the NB and RBFNN methods accomplish worse results whereas the FkNN and DT methods achieve slightly improved results. Along with that, the SOM, RF, SVM, and fuzzy SVM models reached considerable performance.

However, the TDODL-PDR technique outperforms the other recent approaches with maximum CACC and AUC values. Therefore, the TDODL-PDR technique can be employed for accurately classifying and detecting plant ailments.

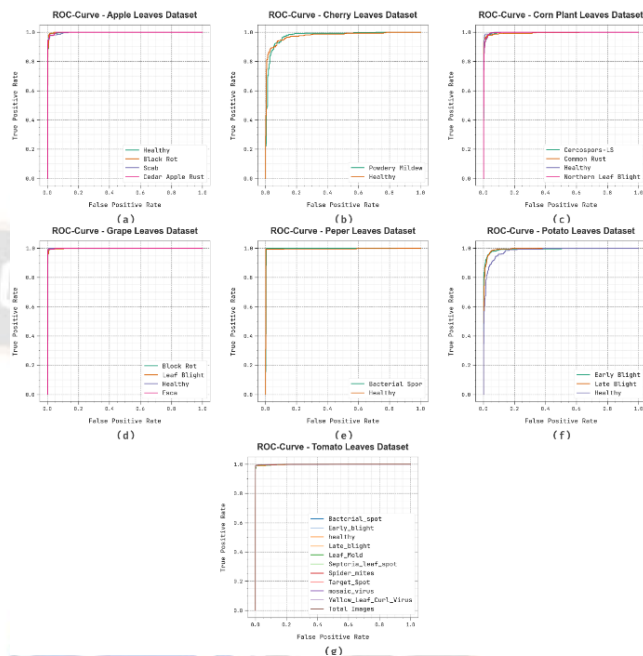


Figure 3. ROC curve of TDODL-PDR approach (a) Apple, (b) Cherry, (c) Corn plant, (d) Grape, (e) Pepper, (f) Potato, and (g) Tomato

TABLE III. TABLE 3 RELATIVE OUTPUT OF TDODL-PDR TECHNIQUE WITH OTHER MODELS UNDER VARIOUS DATASETS

Classifier		NB	RBFNN	FkNN	DT	SOM	RF	SVM	Fuzzy SVM	TDODL-PDR
Apple	CACC	90.10	92.40	95.90	96.50	97.10	97.80	98.40	98.90	99.11
	AUC	93.70	94.50	97.60	98.00	98.40	98.90	99.20	99.50	99.80
Cherry	CACC	95.10	95.90	97.70	97.90	98.50	98.90	99.20	99.50	99.89
	AUC	93.20	94.70	96.50	96.90	97.40	98.00	98.50	99.10	99.46
Corn	CACC	90.90	91.40	92.80	93.30	93.80	94.50	94.90	95.60	98.07
	AUC	91.80	92.20	93.70	94.30	94.70	95.50	96.10	96.70	97.50
Grapes	CACC	92.70	93.30	94.90	95.30	95.70	96.30	96.70	97.10	97.93
	AUC	90.60	91.80	92.70	93.30	93.70	94.40	95.10	95.90	96.99
Pepper	CACC	95.10	95.70	97.30	97.70	98.30	98.80	99.10	99.40	99.71
	AUC	90.80	92.40	93.50	93.90	94.50	95.10	95.50	96.20	97.73
Potato	CACC	90.50	91.30	92.80	93.20	93.60	94.10	94.60	95.10	96.11
	AUC	91.30	92.20	93.40	93.90	94.40	94.90	95.30	95.70	96.49
Tomato	CACC	87.20	88.10	89.10	89.80	90.40	91.30	91.90	92.40	94.46
	AUC	90.20	90.60	91.70	92.30	92.70	93.20	93.70	94.20	95.95

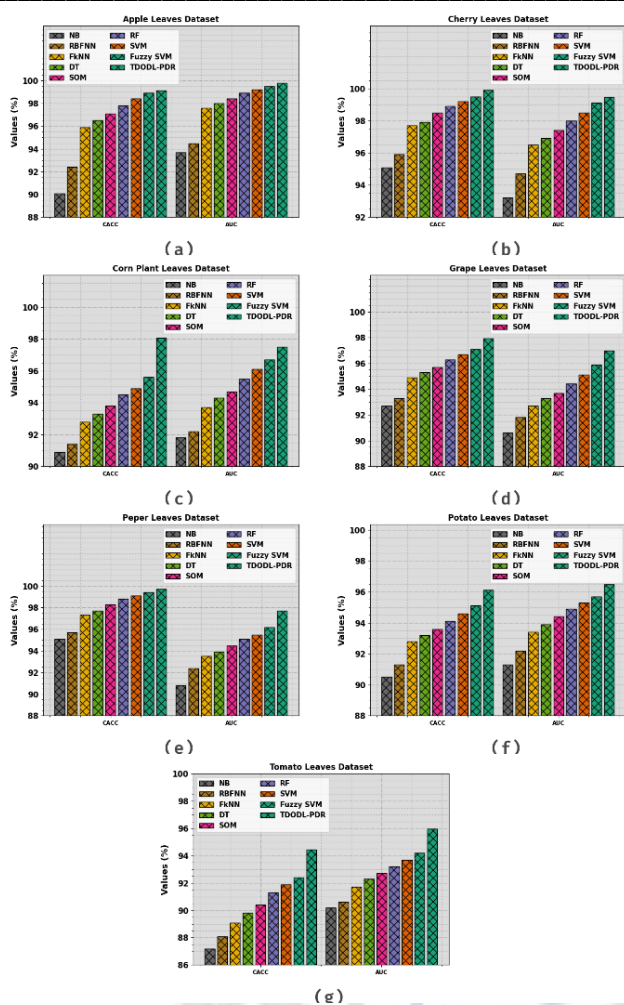


Figure 4. Comparative outcome of TDODL-PDR approach (a) Apple, (b) Cherry, (c) Corn plant, (d) Grape, (e) Pepper, (f) Potato, and (g) Tomato

V. CONCLUSION

In this paper, focus is given on the development of the TDODL-PDR technique for the accurate and automated recognition of PLDs. The TDODL-PDR technique mainly aims to accomplish enhanced crop productivity by reducing crop losses. In addition, the TDODL-PDR technique makes use of the MDLDPTS technique for the feature extraction process, and the BiLSTM model is applied for classification purposes. At last, the TDO approach was utilized for the optimum selection of hyperparameter of the BiLSTM approach. The TDO inspired by the foraging behaviour of TDs effectively explores the parameter space and improves the model's performance. The experimental values stated that the TDODL-PDR model successfully distinguishes healthy plants from diseased ones and accurately classifies different disease types. The automated TDODL-PDR technique offers a practical and reliable solution for early disease detection in crops, enabling farmers to take prompt actions to mitigate the spread and minimize crop losses.

REFERENCES

- [1] A.V. Panchal, S.C. Patel, K. Bagyalakshmi, P. Kumar, I.R. Khan et al., "Image-based plant diseases detection using deep learning," *Materials Today: Proceedings*, vol. 80, pp. 3500-3506, 2023.
- [2] R. Mahum, H. Munir, Z.U.N. Mughal, M. Awais, F. Sher Khan et al., "A novel framework for potato leaf disease detection using an efficient deep learning model," *Human and Ecological Risk Assessment: An International Journal*, pp. 1-24, 2022, doi: 10.1080/10807039.2022.2064814.s
- [3] K. Adem, M.M. Ozguven and Z. Altas, "A sugar beet leaf disease classification method based on image processing and deep learning," *Multimedia Tools and Applications*, vol. 82, no. 8, pp. 12577-12594, 2023.
- [4] R.K. Singh, A. Tiwari and R.K. Gupta, "Deep transfer modeling for classification of maize plant leaf disease," *Multimedia Tools and Applications*, vol. 81, no. 5, pp. 6051-6067, 2022.
- [5] Yaseen Alkubaisi, A. N. ., Abbas Abood, E. ., & Mohammed, M. H. . (2023). Computational Modelling Applications for the Optimal Design of Prefabricated Industrial Buildings According to the Harmonious Research Method . *International Journal of Intelligent Systems and Applications in Engineering*, 11(4s), 302–312. Retrieved from <https://ijisae.org/index.php/IJISAE/article/view/2668>.
- [6] R. Ramamoorthy, E. Saravana Kumar, R.C.A. Naidu and K. Shruthi, "Reliable and Accurate Plant Leaf Disease Detection with Treatment Suggestions Using Enhanced Deep Learning Techniques," *SN Computer Science*, vol. 4, no. 2, p. 158, 2023.
- [7] S. Ashwinkumar, S. Rajagopal, V. Manimaran and B. Jegajothi, "Automated plant leaf disease detection and classification using optimal MobileNet based convolutional neural networks," *Materials Today: Proceedings*, vol. 51, pp. 480-487, 2022.
- [8] Mr. Ashish Uplenchwar. (2017). Modern Speech Identification Model using Acoustic Neural approach . *International Journal of New Practices in Management and Engineering*, 6(03), 01 - 06. <https://doi.org/10.17762/ijnpme.v6i03.58>.
- [9] M. Prabu and B.J. Chelliah, "Mango leaf disease identification and classification using a CNN architecture optimized by crossover-based levy flight distribution algorithm," *Neural Computing and Applications*, vol. 34, no. 9, pp. 7311-7324, 2022.
- [10] R. Sujatha, J.M. Chatterjee, N.Z. Jhanjhi and S.N. Brohi, "Performance of deep learning vs machine learning in plant leaf disease detection," *Microprocessors and Microsystems*, vol. 80, p. 103615, 2021.
- [11] B. Mohith Kumar, K. Rama Krishna Rao, P. Nagaraj, K. M. Sudar and V. Muneeswaran, "Tobacco Plant Disease Detection and Classification using Deep Convolutional Neural Networks," 2022 International Conference on Sustainable Computing and Data Communication Systems (ICSCDS), Erode, India, 2022, pp. 490-495, doi: 10.1109/ICSCDS53736.2022.9760746.
- [12] B.N. Naik, R. Malmathanraj and P. Palanisamy, "Detection and classification of chilli leaf disease using a squeeze-and-excitation-based CNN model," *Ecological Informatics*, vol. 69, p. 101663, 2022.
- [13] Y.M. Abd Algani, O.J.M. Caro, L.M.R. Bravo, C. Kaur, M.S. Al Ansari et al., "Leaf disease identification and classification using

- optimized deep learning," *Measurement: Sensors*, vol. 25, p. 100643, 2023.
- [14] A. Pal and V. Kumar, "AgriDet: Plant Leaf Disease severity classification using agriculture detection framework," *Engineering Applications of Artificial Intelligence*, vol. 119, p. 105754, 2023.
- [15] S.R. Reddy, G.S. Varma and R.L. Davuluri, "Resnet-based modified red deer optimization with DLCNN classifier for plant disease identification and classification," *Computers and Electrical Engineering*, vol. 105, p. 108492, 2023.
- [16] Brian Moore, Peter Thomas, Giovanni Rossi, Anna Kowalska, Manuel López. *Machine Learning for Fraud Detection and Decision Making in Financial Systems*. *Kuwait Journal of Machine Learning*, 2(4). Retrieved from <http://kuwaitjournals.com/index.php/kjml/article/view/216>.
- [17] O. Attallah, "Tomato leaf disease classification via compact convolutional neural networks with transfer learnin, feature selection," *Horticulturae*, vol. 9, no. 2, p. 149, 2023.
- [18] P. Kaur, S. Harnal, V. Gautam, M.P. Singh and S.P. Singh, "A novel transfer deep learning method for detection and classification of plant leaf disease," *Journal of Ambient Intelligence and Humanized Computing*, pp. 1-18, 2022, doi: 10.1007/s12652-022-04331-9.
- [19] J.A. Pandian, K. Kanchanadevi, V.D. Kumar, E. Jasińska, R. Goño et al., "A five convolutional layer deep convolutional neural network for plant leaf disease detection," *Electronics*, vol. 11, no. 8, p. 1266, 2022.
- [20] S. Ashwinkumar, S. Rajagopal, V. Manimaran and B. Jegajothi, "Automated plant leaf disease detection and classification using optimal MobileNet based convolutional neural networks," *Materials Today: Proceedings*, vol. 51, pp. 480-487, 2022.
- [21] N. Venkatakrishnan and M. Natarajan, "Comparative Study of Various Machine Learning Algorithms with MDLDPTS for Plant Leaf Disease Analysis," In *ventive Computation and Information Technologies: Proceedings of ICICIT 2022*, pp. 543-561, 2023, doi: 10.1007/978-981-19-7402-1_39.
- [22] N. Mughees, M.H. Jaffery, A. Mughees, A. Mughees and K. Ejsmont, "Bi-LSTM-Based Deep Stacked Sequence-to-Sequence Autoencoder for Forecasting Solar Irradiation and Wind Speed," *Computers, Materials & Continua*, vol. 75, no. 3, 2023.
- [23] M. Dehghani, Š. Hubálovský and P. Trojovský, "Tasmanian devil optimization: a new bio-inspired optimization algorithm for solving optimization algorithm," *IEEE Access*, vol. 10, pp. 19599-19620, 2022.
- [24] M. Thirunavukkarasu, H. Lala and Y. Sawle, "Reliability index based optimal sizing and statistical performance analysis of stand-alone hybrid renewable energy system using metaheuristic algorithms," *Alexandria Engineering Journal*, vol. 74, pp. 387-413, 2023.
- [25] <https://www.kaggle.com/datasets/emmarex/plantdisease>